

Synthesis and Structures of $P_2(BNR_2)_3$ CagesDanan Dou,[†] Gary L. Wood,[†] Eileen Duesler,[†] Robert T. Paine,^{*†} and Heinrich Nöth^{*†}

Department of Chemistry, University of New Mexico, Albuquerque, New Mexico 87131, and Institut für Anorganische Chemie, Universität München, 8000-München 2, FRG

Received February 19, 1992

The reaction of $(i\text{-Pr}_2\text{N})\text{B}(\text{Cl})\text{P}(\text{SiMe}_3)_2$ with $(i\text{-Pr}_2\text{N})\text{BCl}_2$ in a 2:1 ratio results in the formation of a trigonal-bipyramidal compound, $P_2(i\text{-Pr}_2\text{NB})_3$. A more controlled, predictable synthesis of related P_2B_3 cages is available from reactions of 1,3,2,4-diphosphadiboretanes $(\text{HPBNR}_2)_2$ with $n\text{-BuLi}$, followed by addition of $R_2\text{NBCl}_2$ and then $t\text{-BuLi}$. In this fashion, compounds with the formulas $P_2(i\text{-Pr}_2\text{NB})_2(\text{Btmp})$, $P_2(i\text{-Pr}_2\text{NB})_2[(\text{Me}_3\text{Si})_2\text{NB}]$, $P_2(\text{tmpB})_3$, $P_2(\text{tmpB})_2(i\text{-Pr}_2\text{NB})$, and $P_2(\text{tmpB})_2[(\text{Me}_3\text{Si})_2\text{NB}]$ have been prepared in good yield. Coordination complexes $P_2(i\text{-Pr}_2\text{NB})_2(\text{tmpB})\text{-Cr}(\text{CO})_5$, $P_2(i\text{-Pr}_2\text{NB})_2[(\text{Me}_3\text{Si})_2\text{NB}]\text{-Fe}(\text{CO})_4$, and $P_2(\text{tmpB})_2(i\text{-Pr}_2\text{NB})\text{-Fe}(\text{CO})_4$ have been synthesized; however, attempts to obtain bismetall carbonyl complexes of these ligands or monometal carbonyl complexes of $P_2(\text{Btmp})_3$ were unsuccessful. Molecular structure determinations for two ligands and one complex have been completed by single-crystal X-ray diffraction techniques: $P_2(i\text{-Pr}_2\text{NB})_2[(\text{Me}_3\text{Si})_2\text{NB}]$ ($\text{C}_{18}\text{H}_{46}\text{B}_3\text{N}_3\text{P}_2\text{Si}_2$) crystallizes in the monoclinic space group $P2_1/c$ with $a = 17.782$ (5) Å, $b = 10.098$ (2) Å, $c = 16.826$ (4) Å, $\beta = 90.58$ (2)°, and $Z = 4$; $P_2(\text{tmpB})_3$ ($\text{C}_{27}\text{H}_{54}\text{B}_3\text{N}_3\text{P}_2$) crystallizes in the hexagonal space group $P6(3)/m$ with $a = 10.9085$ (15) Å, $c = 14.948$ (3) Å, and $Z = 2$; $P_2(i\text{-Pr}_2\text{NB})_2(\text{tmpB})\text{-Cr}(\text{CO})_5$ ($\text{C}_{26}\text{H}_{46}\text{B}_3\text{N}_3\text{O}_5\text{P}_2\text{Cr}$) crystallizes in the triclinic space group $P\bar{1}$ with $a = 11.548$ (5) Å, $b = 16.525$ (5) Å, $c = 19.911$ (8) Å, $\alpha = 104.85$ (3)°, $\beta = 105.87$ (3)°, $\gamma = 92.57$ (3)°, and $Z = 4$. The structural parameters for these ligands and the metal complex are compared with parametric data from several diphosphadiboretane ligands and complexes.

Introduction

Cage and cluster compounds formed with boron and carbon (carboranes and metallocarboranes) are well known, and their chemistry has been extensively developed.¹ Cages formed by boron and other main-group elements, on the other hand, are relatively few, and their chemistry has not been examined in detail.² For the combination of boron and phosphorus, the development of cage compounds has been hindered by a lack of appropriate precursor compounds for cage construction reactions.³ In the last few years, however, this situation has begun to change, and a few cage compounds have appeared. For example, Nöth and co-workers⁴ have observed that photolysis of the diphosphadiboretanes $(R_2\text{NBPCEt}_3)_2$ ($R_2\text{N} = \text{tmp},^5 t\text{-Bu}_2\text{N}$) leads to tetrahedrane clusters $(R_2\text{NBP})_2$, and efforts are in progress to determine factors that will generalize this photochemical reaction from other precursors. In another approach, thermolysis of a 2:1 mixture of $(i\text{-Pr}_2\text{N})\text{B}(\text{Cl})\text{P}(\text{SiMe}_3)_2$ and $i\text{-Pr}_2\text{NBCl}_2$ leads to formation of a trigonal-bipyramidal cage compound⁶ $P_2(i\text{-Pr}_2\text{NB})_3$. Unfortunately, this reaction is not general, and efforts to develop better synthetic processes continue. In this paper, we describe a stepwise synthesis for additional examples of $P_2(R_2\text{NB})_3$ and $P_2(R_2\text{NB})_2(R_2'\text{NB})$ compounds that utilizes readily

available lithium salts of diphosphadiboretanes $(R_2\text{NBPH})_2$. Selected coordination chemistry of the cages is also summarized.

Experimental Section

General Information. Standard inert-atmosphere techniques were used for the manipulation of all reagents and reaction products. Infrared spectra were recorded on Nicolet 6000 or Matteson 2020 FT-IR spectrometers from solution cells or KBr pellets. Mass spectra were obtained from a Finnegan mass spectrometer by using a GC inlet system or heated solids probe. NMR spectra were recorded on Bruker WP-250 and JEOL GSX-400 spectrometers. All NMR samples were sealed in 5-mm tubes with deuterated lock solvent, and the spectra were referenced with Me_4Si (^{13}C , ^1H), $\text{BF}_3\cdot\text{Et}_2\text{O}$ (^{11}B), and 85% H_3PO_4 (^{31}P). Elemental analyses were from the UNM analytical services laboratory.

Materials. Reagents $i\text{-Pr}_2\text{NBCl}_2$,⁷ tmpBCl_2 ,⁸ $(\text{Me}_3\text{Si})_2\text{NBCl}_2$,⁹ $\text{LiPH}_2\text{-DME}$,¹⁰ the diphosphadiboretanes $(i\text{-Pr}_2\text{NBPH})_2$, **1**, and $(\text{tmpBPH})_2$,^{9,4,11} their lithium salts **2** and **10**,¹¹ and $\text{Cr}(\text{CO})_5\text{-NMe}_3$ ¹² were prepared as described in the literature. The $n\text{-BuLi}$ and $t\text{-BuLi}$ solutions (Aldrich) were purchased and used as received. Solvents were dried and degassed by standard methods, and solvent transfers were accomplished by vacuum distillation.

Synthesis and Characterization of Compounds. **2,4-Bis(diisopropylamino)-1-[chloro(2,2,6,6-tetramethylpiperidino)boryl]-1,3,2,4-diphosphadiboretane (3).** A 1.9-g (5.0-mmol) sample of **2** dissolved in 25 mL of hexane was added to 1.2 g (5.0 mmol) of tmpBCl_2 in 25 mL of hexane held at -78°C . The mixture was stirred at -78°C for 2 h, warmed to 23°C , and stirred for an additional 15 h. The resulting yellow, cloudy solution was filtered, and the filtrate was vacuum evaporated, leaving a yellow oil. No further purification was required. Yield: 2.3 g (97%). Mass spectrum (30 ev): m/e (%) = 471 (30, M^+), 293 (100). Infrared spectrum (cyclohexane, cm^{-1}): 2256 (w), 2236 (w), 1472 (m), 1459 (m), 1444 (m), 1367 (s), 1316 (s), 1303 (s), 1185 (m), 1166 (m), 1150 (m),

[†] University of New Mexico.[†] Universität München.

- (1) Grimes, R. N. *Carboranes*; Academic Press: New York, 1970. Beall, H. In *Boron Hydride Chemistry*; Muettterties, E. L., Ed.; Academic Press: New York, 1975; Chapter 9. Onak, T. *Ibid.*; Chapter 10. Dunks, G. B.; Hawthorne, M. F. *Ibid.*; Chapter 11. Callahan, K. P.; Hawthorne, M. F. *Adv. Organomet. Chem.* **1976**, *14*, 145. Grimes, R. N. *Pure Appl. Chem.* **1974**, *39*, 455. Callahan, K. P.; Hawthorne, M. F. *Ibid.* **1974**, *39*, 475.
- (2) Sowerby, D. B. In *The Chemistry of Inorganic Homo- and Heterocycles*; Haiduc, I.; Scowberby, D. B., Eds.; Academic Press: New York, 1987; Vol. I, Chapter 3.
- (3) Power, P. P. *Angew. Chem., Int. Ed. Engl.* **1990**, *29*, 449.
- (4) Kölle, P.; Linti, G.; Nöth, H.; Polborn, K. J. *Organomet. Chem.* **1988**, *355*, 7.
- (5) Abbreviations used in the text include tmp = 2,2,6,6-tetramethylpiperidino, Me = methyl, tms = trimethylsilyl, THF = tetrahydrofuran, $i\text{-Pr}$ = isopropyl, and DME = ethylene glycol dimethyl ether.
- (6) Wood, G. L.; Duesler, E. N.; Narula, C. K.; Paine, R. T.; Nöth, H. J. *Chem. Soc., Chem. Commun.* **1987**, 496.

(7) Gerrard, W.; Hudson, H. R.; Mooney, E. R. *J. Chem. Soc.* **1960**, 5168.(8) Nöth, H.; Weber, S. Z. *Naturforsch., B* **1983**, *37*, 1460.(9) $(\text{tms})_2\text{NBCl}_2$ was prepared by a modification of the literature method: Geymayer, P.; Rochow, E. G. *Monatsh. Chem.* **1966**, *97*, 429.(10) Schäfer, H.; Fritz, G.; Hölderich, W. Z. *Anorg. Allg. Chem.* **1977**, *428*, 222.(11) Dou, D.; Westerhausen, M.; Wood, G. L.; Linti, G.; Duesler, E. N.; Nöth, H.; Paine, R. T. *Chem. Ber.*, submitted for publication.(12) Wasserman, H. J.; Workulich, M. J.; Atwood, J. D.; Churchill, M. R. *Inorg. Chem.* **1980**, *19*, 2831.

1139 (m), 1002 (w), 875 (w), 808 (w). Anal. Calcd for C₂₁H₄₇B₃N₃P₂Cl (471.46): C, 53.50; H, 10.05; N, 8.91. Found: C, 53.14; H, 10.18; N, 8.26.

2,4-Bis(diisopropylamino)-5-(2,2,6,6-tetramethylpiperidino)-1,3-diphospha-2,4,5-triborabicyclo[1.1.1]pentane (4). A sample of 3 (1.7 g, 3.6 mmol) was dissolved in 50 mL of hexane, the solution was cooled to -78 °C, and 2.1 mL of *t*-BuLi (1.7 M) was added dropwise with stirring. The mixture was then warmed to 23 °C over 2 h and stirred for an additional 16 h. The resulting orange, cloudy solution was filtered, the filtrate vacuum evaporated, and the residue recrystallized twice from hexane at -10 °C, leaving a white crystalline solid. Yield: 0.80 g (51%). The dehydrohalogenation may also be accomplished with *n*-BuLi by refluxing the reaction mixture for 2 days; however, the yield of 4 is reduced to ~31%. Mp: 179–182 °C. Mass spectrum (30 eV): *m/e* (%) = 435 (100, M⁺). Infrared spectrum (hexane, cm⁻¹): 1435 (s), 1366 (s), 1327 (s), 1304 (vs), 1188 (m), 1150 (m), 1009 (w), 573 (w). Anal. Calcd for C₂₁H₄₆B₃N₃P₂ (435.0): C, 57.98; H, 10.66; N, 9.66. Found: C, 57.92; H, 10.96; N, 9.86.

2,4-Bis(diisopropylamino)-1-[chloro[bis(trimethylsilyl)amino]boryl]-1,3,2,4-diphosphadiboretane (5). A sample of 2 (0.55 g, 1.4 mmol) was dissolved in 25 mL of hexane, and this was added to a solution containing 0.35 g (1.4 mmol) of (Me₃Si)₂NBCl₂ in 25 mL of hexane held at 23 °C. The mixture was stirred for 1 week and filtered and the filtrate vacuum evaporated. The residue was recrystallized twice from a minimum of hexane held at -10 °C, leaving colorless crystals. Yield: 0.30 g (44%). Mp: 105–107 °C dec. Mass spectrum (30 eV): *m/e* (%) = 492 (20, M⁺), 313 (100), 110 (100), 98 (100). Infrared spectrum (hexane, cm⁻¹): 2266 (w), 1478 (w), 1444 (m), 1368 (m), 1314 (s), 1252 (s), 1186 (s), 1152 (m), 1117 (w), 1007 (w), 907 (s), 868 (s), 847 (s), 789 (w), 768 (w), 737 (w). Anal. Calcd for C₁₈H₄₇B₃N₃Si₂P₂Cl (491.6): C, 43.98; H, 9.64; N, 8.55. Found: C, 43.58; H, 9.92; N, 8.82.

2,4-Bis(diisopropylamino)-5-[bis(trimethylsilyl)amino]-1,3-diphospha-2,4,5-triborabicyclo[1.1.1]pentane (6). A sample of 5 (3.3 mmol) was prepared as described above, and without isolation, it was combined slowly at -78 °C with 1.9 mL of *t*-BuLi (1.7 M). The solution immediately turned cloudy and orange-brown. After stirring overnight, the solution was filtered and the solvent removed by vacuum evaporation. The residue was recrystallized twice from hexane at -10 °C, and colorless crystals were collected. Yield: 0.70 g (47%). Mp: 114–116 °C. Mass spectrum (30 eV): *m/e* (%) = 455 (85, M⁺), 342 (100), 253 (25), 181 (20), 126 (30), 110 (35), 98 (40). Infrared spectrum (hexane, cm⁻¹): 1435 (m), 1366 (m), 1302 (s), 1250 (s), 1207 (s), 1188 (s), 1150 (m), 1009 (m), 928 (m), 910 (m), 868 (vs), 846 (s), 761 (w), 737 (w), 570 (w). Anal. Calcd for C₁₈H₄₆B₃N₃Si₂P₂ (455.14): C, 47.50; H, 10.19; N, 9.23. Found: C, 47.59; H, 10.47; N, 9.28.

2,4,5-Tris(diisopropylamino)-1,3-diphospha-2,4,5-triborabicyclo[1.1.1]pentane (8). A sample of 2 (1.2 g, 3.2 mmol) was added at -78 °C to 0.57 g (3.2 mmol) of *i*-Pr₂NBCl₂ dissolved in 50 mL of hexane. The reaction mixture was stirred at -78 °C for 2 h, then warmed to 23 °C, and stirred for an additional 16 h. The resulting cloudy, yellow solution was filtered, and 1.84 mL (1.7 M) of *t*-BuLi was added to the filtrate at -78 °C. The mixture was held at -78 °C for 2 h and then stirred at 23 °C for 16 h. The cloudy, yellow solution was filtered, and solvent evaporated from the filtrate, and the remaining residue recrystallized twice from hexane at -10 °C, leaving a yellow crystalline solid. Yield: 0.50 g (40%). Mp: 124–126 °C. Mass spectrum (70 eV): *m/e* (%) = 394 (M⁺, 100), 352 (M⁺ - *i*-Pr₂). Infrared spectrum (CH₂Cl₂, cm⁻¹): 1467 (m), 1434 (s), 1378 (w), 1365 (m), 1303 (s), 1253 (w), 1187 (w), 1145 (m), 1110 (w), 1010 (w), 809 (w), 796 (w), 571 (w). Anal. Calcd for C₁₈H₄₂B₃N₃P₂ (394.93): C, 54.74; H, 10.72; N, 10.64. Found: C, 54.77; H, 10.96; N, 10.67.

2,4-Bis(2,2,6,6-tetramethylpiperidino)-1-[chloro(diisopropylamino)boryl]-1,3,2,4-diphosphadiboretane (11). A suspension containing 1.9 g (4.2 mmol) of 10 in 25 mL of hexane was added to *i*-Pr₂NBCl₂ (0.76 g, 4.2 mmol) in 25 mL of hexane cooled to -78 °C. The mixture was stirred for 2 h, then warmed to 23 °C, and stirred for an additional 16 h. The mixture was then heated to 50 °C and stirred for 5 h. The resulting mixture was filtered, the solvent removed by vacuum evaporation, and the residue recrystallized from hexane at -10 °C, leaving colorless crystals. Yield: 1.0 g (47%). Mp: 122–125 °C. Mass spectrum (30 eV): *m/e* (%) = 511 (3, M⁺), 475 (7), 333 (40), 126 (40), 69 (100). Infrared spectrum (cyclohexane, cm⁻¹): 2246 (w), 2232 (w), 1381 (m), 1368 (s), 1319 (s), 1300 (s), 1169 (m), 1132 (w), 998 (w). Anal. Calcd for C₂₄H₅₁B₃N₃P₂Cl (511.52): C, 56.35; H, 10.05; N, 8.21. Found: C, 56.31; H, 10.44; N, 8.04.

2,4-Bis(2,2,6,6-tetramethylpiperidino)-5-(diisopropylamino)-1,3-diphospha-2,4,5-triborabicyclo[1.1.1]pentane (12). A suspension of 1.8 g

(3.8 mmol) of 10 in 50 mL of hexane was cooled to -78 °C, and a solution containing 0.71 g (3.8 mmol) of *i*-Pr₂NBCl₂ in 50 mL of hexane was added with stirring. The mixture was stirred for 3 h, warmed to 23 °C for 3 h, and then warmed to 50 °C for 5 h. The resulting yellow, cloudy mixture was filtered and 2.3 mL (1.7 M) of *t*-BuLi added slowly to the filtrate at -78 °C. The mixture was held at -78 °C for 2 h, then warmed to 23 °C, and stirred for 16 h. The orange-colored solution was filtered, the solvent removed by vacuum evaporation, and the residue recrystallized twice from hexane at -10 °C, leaving colorless crystals. Yield: 1.2 g (66%). The dehydrohalogenation may also be accomplished with *n*-BuLi under reflux with decreased yield (~44%). Mp: 177–179 °C. Mass spectrum (30 eV): *m/e* (%) = 475 (100, M⁺), 293 (30). Infrared spectrum (hexane, cm⁻¹): 1435 (m), 1365 (vs), 1327 (s), 1312 (s), 1292 (s), 1258 (w), 1244 (w), 1186 (m), 1163 (m), 1132 (m), 1009 (w), 989 (w). Anal. Calcd for C₂₄H₅₀B₃N₃P₂ (475.06): C, 60.68; H, 10.61; N, 8.84. Found: C, 60.89; H, 10.88; N, 8.39.

2,4-Bis(2,2,6,6-tetramethylpiperidino)-5-[bis(trimethylsilyl)amino]-1,3-diphospha-2,4,5-triborabicyclo[1.1.1]pentane (13). The compound was prepared from the combination of 1.0 g (2.1 mmol) of 10 in 25 mL of hexane and 0.52 g (2.1 mmol) of (Me₃Si)₂NBCl₂ in 25 mL of hexane held at -78 °C. The mixture was stirred for 4 h, warmed at 23 °C, stirred for an additional 16 h, and then heated at 50 °C for 5 h. The cloudy, yellow solution was filtered, the solvent vacuum evaporated, and the residue recrystallized twice from hexane at -10 °C, leaving colorless crystals. Yield: 0.10 g (8.7%). Mp: 182–184 °C. Mass spectrum (30 eV): *m/e* (%) = 535 (30, M⁺), 353 (30), 146 (40), 126 (70), 69 (100). Infrared spectrum (cyclohexane, cm⁻¹): 1385 (s), 1381 (m), 1326 (s), 1291 (m), 1250 (s), 1213 (m), 1172 (m), 925 (m), 867 (s), 846 (s), 729 (w). Anal. Calcd for C₂₄H₅₄B₃N₃P₂Si₂ (535.27): C, 53.85; H, 10.17; N, 7.85. Found: C, 53.35; H, 10.44; N, 7.82. Samples of the colorless crystals are contained yellow, crystalline (tmpBP)₂, which was identified by its NMR spectra.⁴

2,4,5-Tris(2,2,6,6-tetramethylpiperidino)-1,3-diphospha-2,4,5-triborabicyclo[1.1.1]pentane (14). A solution containing 0.50 g (1.1 mmol) of 10 in 25 mL of hexane was added to 0.24 g (1.1 mmol) of tmpBCl₂ in 25 mL of hexane held at 0 °C. The mixture was stirred for 2 h, warmed to 23 °C, and stirred for 20 h. The resulting cloudy, yellow mixture was filtered. The solvent was vacuum evaporated from the filtrate and the yellow residue recrystallized from hexane at room temperature, leaving yellow crystals. Yield: 0.35 g (63%). Mp: 254–256 °C. Mass spectrum (30 eV): *m/e* (%) = 515 (90, M⁺), 333 (100), 69 (95). Infrared spectrum (hexane, cm⁻¹): 1464 (w), 1452 (s), 1366 (s), 1327 (s), 1292 (m), 1258 (w), 1244 (w), 1165 (m), 1130 (w), 1005 (w), 989 (w), 974 (w). Anal. Calcd for C₂₇H₅₄B₃N₃P₂ (515.13): C, 62.95; H, 10.57; N, 8.16. Found: C, 63.01; H, 10.92; N, 8.73.

[2,4-Bis(diisopropylamino)-5-(2,2,6,6-tetramethylpiperidino)-1,3-diphospha-2,4,5-triborabicyclo[1.1.1]pentane]chromium Pentacarbonyl (15). A sample of 4 (0.20 g, 0.46 mmol) was dissolved in 25 mL of hexane and the solution combined with 0.12 g (0.46 mmol) of Cr(CO)₅-NMe₂ dissolved in 25 mL of hexane. The mixture was stirred for 16 h at 23 °C, the solvent evaporated, and the residue recrystallized from hexane at -10 °C, leaving yellow crystals. Yield: 0.15 g (52%). Mp: 144–147 °C. Mass spectrum (30 eV): *m/e* (%) = 487 (8), 475 (5), 435 (100), 336 (47), 151 (30), 110 (13). Infrared spectrum (cyclohexane, cm⁻¹): 2053 (s), 1954 (s), 1934 (vs), 1472 (m), 1367 (m), 1315 (m), 855 (m), 672 (m). Anal. Calcd for C₂₆H₄₆B₃N₃O₅P₂Cr (627.05): C, 49.80; H, 7.39; N, 6.70. Found: C, 49.27; H, 7.70; N, 6.48.

[2,4-Bis(diisopropylamino)-5-[bis(trimethylsilyl)amino]-1,3-diphospha-2,4,5-triborabicyclo[1.1.1]pentane]iron Tetracarbonyl (16). A solution containing 0.39 g (0.86 mmol) of 6 in 25 mL of hexane was combined with 0.31 g (0.86 mmol) of Fe₂(CO)₉ in 25 mL of hexane at 23 °C, and the mixture was stirred for 1 week. The resulting brown solution was filtered, the solvent removed by vacuum evaporation, and the residue recrystallized from hexane at -10 °C, leaving yellow brown crystals. Yield: 0.30 g (56%). Mp: 147–150 °C dec. Mass spectrum (30 eV): *m/e* (%) = 623 (0.5, M⁺), 567 (15), 511 (90), 455 (25), 398 (30), 342 (45), 256 (30), 227 (70), 217 (40), 179 (100). Infrared spectrum (hexane, cm⁻¹): 2041 (s), 1966 (s), 1935 (vs), 1477 (w), 1369 (w), 1319 (w), 1254 (m), 899 (w), 866 (w), 851 (w), 621 (m). Anal. Calcd for C₂₂H₄₆B₃N₃O₄P₂Si₂Fe (623.02): C, 42.41; H, 7.44; N, 6.74. Found: C, 42.35; H, 7.70; N, 6.90.

[2,4-Bis(2,2,6,6-tetramethylpiperidino)-5-(diisopropylamino)-1,3-diphospha-2,4,5-triborabicyclo[1.1.1]pentane]iron Tetracarbonyl (17). A solution containing 0.35 g (0.74 mmol) of 12 in 25 mL of hexane was combined with 0.27 g (0.74 mmol) of Fe₂(CO)₉ in 25 mL of hexane at 23 °C, and the mixture was stirred for 6 days. The resulting red-brown solution was filtered, the solvent removed by vacuum evaporation, and the solid residue recrystallized from hexane at -10 °C, leaving brown

Table I. Crystallographic Data for $P_2(i-Pr_2NB)_2[(Me_3Si)_2NB]$, **6**, $P_2(tmpB)_3$, **14**, and $P_2(i-Pr_2NB)_2(tmpB) \cdot Cr(CO)_5$, **15**

	6	14	15
chemical formula	$C_{18}H_{46}B_3N_3P_2Si_2$	$C_{27}H_{54}B_3N_3P_2$	$C_{26}H_{46}B_3N_3P_2O_5Cr$
<i>a</i> (Å)	17.782 (5)	10.909 (2)	11.548 (5)
<i>b</i> (Å)	10.098 (2)		16.525 (5)
<i>c</i> (Å)	16.826 (4)	14.948 (3)	19.911 (8)
α (deg)	90	90	104.85 (3)
β (deg)	90.58 (2)	90	105.87 (3)
γ (deg)	90	120	92.57 (3)
<i>V</i> (Å ³)	3021.3 (13)	1540.5 (4)	3505.8
<i>Z</i>	4	2	4
ρ_{calcd} (g cm ⁻³)	1.001	1.11	1.188
formula weight	455.1	515.1	627.0
cryst dimens (mm)	0.14 × 0.37 × 0.50	0.18 × 0.25 × 0.87	0.09 × 0.35 × 0.55
cryst syst	monoclinic	hexagonal	triclinic
space group	$P2_1/c$	$P6(3)/m$	$P\bar{1}$
<i>T</i> (°C)	20°	20°	20°
μ (mm ⁻¹)	0.227	0.156	0.441
2θ range	2–50	2–50	2–37
reflens measd	$\pm h, -k, +l$	$-h, \pm k, +l$	$+h, \pm k, \pm l$
total no. of reflens collected	5992	5945	5596
no. unique reflens	5305	942	5214
no. obsd reflens	2633 ($F > 3\sigma(F)$)	861 ($F > 3\sigma(F)$)	3222 ($F > 3\sigma(F)$)
trans coeff			
min/max	0.5130/0.5249	0.9465/0.9850	0.8657/0.9668
<i>R</i> _F	7.83	10.13	8.40
<i>R</i> _{wF}	6.22	9.44	7.73

crystals. Yield: 0.3 g (63%). Mp: 209–211 °C dec. Mass spectrum (30 eV): *m/e* (%) = 586 (3), 531 (8), 475 (100), 293 (20), 126 (15). Infrared spectrum (hexane, cm⁻¹): 2037 (s) 1962 (s), 1933 (vs), 908 (s) 737 (s), 621 (m). Anal. Calcd for $C_{28}H_{50}B_3N_3O_4P_2Fe$ (642.95): C, 52.31; H, 7.84; N, 6.54. Found: C, 51.51; H, 8.10; N, 6.62.

Crystallographic Measurement and Structure Solutions. Crystals of **6**, **14**, and **15** were placed in glass capillaries under a dry nitrogen atmosphere. The crystals were centered on a Syntex P3/F automated diffractometer, and determinations of crystal class, orientation matrix, and unit cell dimensions were performed in a standard manner. A summary of crystallographic data is given in Table I. Data were collected in the ω scan mode with Mo K α ($\lambda = 0.71069$ Å) radiation, a scintillation counter, and a pulse height analyzer. In each case, inspection of a small data set led to assignment of the indicated space groups.¹³ Empirical adsorption corrections were applied, based on ψ scans.¹⁴ No signs of crystal decay were noted.

All calculations were performed on a Siemens SHELXTL PLUS (Microvax II version) structure determination system.¹⁵ Solutions for the data sets were by direct methods, and full matrix refinements were employed.¹⁶ Neutral atom scattering factors and anomalous dispersion terms were used for all non-hydrogen atoms during the refinements. The function minimized was $\sum w(|F_o| - |F_c|)^2$. The refinements for **6** and **15** were well-behaved. The refinement for **14** was performed in both $P6(3)/m$ and $P6(3)$. Refinement in the noncentric space group gave slightly lower *R* factors; however, the generalized *R* factor, $R_g = 10.38\%$, was higher. Application of Hamilton's statistical tests indicated that the centric space group $P6(3)/m$ is the correct choice. Results in $P6(3)$ also show more disparity among equivalent bond distances, bond angles, and *U*'s for equivalent atoms. Listings of the non-hydrogen atom coordinates are given in Tables II–IV, and a summary of key metrical parameters is provided in Table V. Additional crystallographic parameters and details of the structure solutions (Table S-1), hydrogen atom positional parameters

Table II. Atomic Coordinates ($\times 10^4$) and Their Esd's for $P_2(i-Pr_2NB)_2[(Me_3Si)_2NB]$, **6**

	<i>x</i>	<i>y</i>	<i>z</i>
P(1)	7398 (1)	1282 (2)	1984 (1)
P(2)	7945 (1)	305 (2)	422 (1)
B(1)	7603 (4)	-369 (9)	1443 (4)
B(2)	8288 (4)	1367 (8)	1315 (4)
B(3)	7122 (4)	1356 (7)	857 (4)
N(1)	7533 (3)	-1644 (6)	1732 (3)
N(2)	8979 (3)	1978 (5)	1428 (3)
N(3)	6517 (3)	1995 (5)	465 (2)
C(1)	7279 (5)	-1888 (8)	2568 (4)
C(2)	6555 (5)	-2644 (9)	2593 (5)
C(3)	7896 (5)	-2449 (10)	3081 (4)
C(4)	7708 (4)	-2844 (8)	1279 (5)
C(5)	8521 (5)	-2908 (9)	1035 (5)
C(6)	7185 (5)	-3013 (9)	582 (5)
C(7)	9557 (4)	1952 (8)	797 (5)
C(8)	9780 (5)	3318 (9)	526 (5)
C(9)	10 204 (4)	1049 (9)	1010 (5)
C(10)	9212 (4)	2615 (9)	2179 (5)
C(11)	9285 (4)	1651 (9)	2851 (4)
C(12)	8736 (5)	3803 (9)	2380 (5)
Si(1)	5673 (1)	2240 (2)	985 (1)
C(13)	5519 (3)	871 (8)	1704 (4)
C(14)	4842 (3)	2186 (9)	301 (4)
C(15)	5704 (4)	3844 (8)	1517 (4)
Si(2)	6690 (1)	2514 (2)	-521 (1)
C(16)	6044 (4)	3877 (8)	-830 (4)
C(17)	6597 (4)	1118 (8)	-1214 (3)
C(18)	7647 (4)	3246 (7)	-581 (3)

Table III. Atomic Coordinates ($\times 10^4$) and Their Esd's for $P_2(tmpB)_3$, **14**

	<i>x</i>	<i>y</i>	<i>z</i>
P	6667	3333	1532 (1)
N	4060 (5)	958 (5)	2500
B	5401 (7)	2190 (7)	2500
C(1)	3417 (4)	205 (4)	1624 (3)
C(2)	1837 (6)	-904 (7)	1702 (3)
C(3)	1435 (8)	-1831 (8)	2500
C(4)	4248 (7)	-421 (6)	1249 (3)
C(5)	3407 (5)	1252 (6)	936 (3)

(Table S-5), anisotropic thermal parameters (Table S-4), full listings of bond distances and angles (Tables S-2 and S-3), and listings of structure factor amplitudes are provided in the supplementary material.

Results and Discussion

Previous studies⁶ in our group revealed that thermolysis of a 2:1 mixture of *i*-Pr₂NB(Cl)[P(SiMe₃)₂] and *i*-Pr₂NBCl₂ at 160

(13) Space group notation is given in *International Tables for X-Ray Crystallography*; Reidel: Dordrecht, Holland, 1983; Vol. 1, pp 73–346.

(14) The empirical absorption corrections use an ellipsoidal model fitted to azimuthal scan data that are then applied to the intensity data: *SHELXTL Manual, Revision 4*; Nicolet XRD Corp.: Madison, WI, 1983.

(15) Sheldrick, G. M. *Nicolet SHELXTL Operations Manual*; Nicolet XRD Corp.: Cupertino, CA, 1981. SHELXTL uses absorption, anomalous dispersion, and scattering data compiled in *International Tables for X-Ray Crystallography*; Kynoch: Birmingham, England, 1974; Vol. IV, pp 55–60, 99–101, 149–150. Anomalous dispersion terms were included for all atoms with atomic numbers greater than 2.

(16) A general description of the least-squares algebra is found in *Crystallographic Computing*; Ahmed, F. R., Hall, S. R., Huber, C. P., Eds.; Munksgaard: Copenhagen, 1970; p 187. The least-squares refinement minimizes $\sum w(|F_o| - |F_c|)^2$, where $w = 1/[\sigma(F)^2 + gF^2]$. $R = \sum |F_o| - |F_c| / \sum |F_o|$, $R_w = \{[\sum (|F_o| - |F_c|)^2] / \sum wF_o^2\}^{1/2}$, and GOF $[\sum w(|F_o| - |F_c|)^2 / (NO - NV)]^{1/2}$, where NO = number of observations and NV = number of variables.

Table IV. Atomic Coordinates (×10⁴) and Their Esd's for P₂(*i*-Pr₂NB)₂(tmpB)·Cr(CO)₅, 15

	x	y	z		x	y	z
Cr(1)	-6205 (2)	9243 (2)	1436 (1)	Cr(2)	3289 (2)	3063 (2)	3726 (1)
C(1)	-6006 (13)	8726 (9)	530 (9)	C(6)	3912 (16)	2616 (11)	3005 (10)
O(1)	-5902 (9)	8448 (7)	-44 (6)	O(6)	4463 (11)	2294 (8)	2595 (7)
C(2)	-5472 (14)	10 247 (10)	1392 (8)	C(7)	4245 (15)	2454 (10)	4239 (9)
O(2)	-5038 (10)	10 878 (7)	1350 (6)	O(7)	4869 (10)	2054 (7)	4553 (6)
C(3)	-7687 (15)	9458 (10)	958 (8)	C(8)	4610 (15)	3869 (10)	4008 (8)
O(3)	-8654 (10)	9543 (6)	636 (6)	O(8)	5467 (11)	4358 (7)	4210 (6)
C(4)	-6479 (15)	9880 (11)	2263 (10)	C(9)	2852 (13)	3582 (9)	4562 (8)
O(4)	-6718 (11)	10 312 (8)	2757 (7)	O(9)	2638 (9)	3914 (7)	5090 (6)
C(5)	-6950 (14)	8299 (10)	1566 (8)	C(10)	2102 (15)	2152 (10)	3371 (8)
O(5)	-7450 (10)	7715 (7)	1620 (6)	O(10)	1368 (11)	1579 (8)	3177 (6)
P(1)	-4310 (3)	8699 (2)	1969 (2)	P(3)	1715 (3)	3779 (2)	3037 (2)
P(2)	-2213 (3)	7888 (2)	2423 (2)	P(4)	-312 (3)	4398 (3)	2212 (2)
B(1)	-3168 (13)	8617 (9)	2882 (8)	B(4)	1292 (14)	4871 (10)	2862 (8)
N(1)	-2993 (9)	9012 (7)	3635 (6)	N(4)	1894 (10)	5683 (7)	3082 (5)
C(11)	-3493 (13)	9823 (9)	3895 (8)	C(41)	1146 (14)	6444 (10)	3037 (8)
C(12)	-2646 (16)	10 333 (11)	4670 (9)	C(42)	1924 (16)	7235 (11)	3618 (10)
C(13)	-2404 (17)	9850 (12)	5214 (10)	C(43)	3139 (17)	7413 (12)	3544 (10)
C(14)	-2533 (16)	8942 (11)	4946 (9)	C(44)	3685 (16)	6682 (11)	3173 (10)
C(15)	-2258 (14)	8617 (10)	4196 (8)	C(45)	3267 (14)	5836 (10)	3314 (8)
C(16)	-3521 (13)	10 392 (9)	3419 (7)	C(46)	61 (14)	6327 (9)	3278 (8)
C(17)	-4770 (14)	9637 (10)	3962 (8)	C(47)	810 (14)	6507 (9)	2275 (8)
C(18)	-2576 (14)	7677 (9)	3972 (8)	C(48)	3801 (13)	5155 (9)	2869 (8)
C(19)	-898 (13)	8822 (10)	4305 (8)	C(49)	3687 (14)	5885 (10)	4121 (8)
B(2)	-2647 (14)	8762 (10)	1931 (8)	B(5)	6 (14)	3824 (10)	2961 (8)
N(2)	-1986 (9)	9236 (6)	1666 (5)	N(5)	-777 (10)	3548 (6)	3302 (6)
C(21)	-661 (13)	9191 (9)	1710 (8)	C(51)	-2082 (14)	3643 (10)	3134 (8)
C(22)	-514 (14)	8322 (9)	1265 (8)	C(52)	-2292 (15)	4564 (9)	3317 (8)
C(23)	101 (14)	9408 (10)	2483 (8)	C(53)	-2777 (15)	3180 (10)	2354 (8)
C(24)	-2584 (13)	9840 (9)	1276 (7)	C(54)	-311 (14)	3145 (9)	3896 (8)
C(25)	-1980 (15)	10 722 (10)	1638 (9)	C(55)	-402 (15)	3687 (10)	4613 (8)
C(26)	-2633 (15)	9556 (10)	472 (8)	C(56)	-980 (14)	2263 (9)	3735 (8)
B(3)	-3830 (14)	7576 (10)	1747 (8)	B(6)	814 (16)	3628 (11)	2025 (10)
N(3)	-4346 (9)	6801 (7)	1238 (5)	N(6)	1011 (10)	3161 (7)	1389 (6)
C(31)	-3699 (13)	6021 (9)	1165 (8)	C(61)	198 (14)	3112 (10)	629 (9)
C(32)	-2590 (14)	6117 (9)	958 (8)	C(62)	287 (15)	3952 (10)	482 (9)
C(33)	-3521 (13)	5728 (9)	1843 (8)	C(63)	-1075 (14)	2757 (10)	535 (9)
C(34)	-5555 (12)	6676 (9)	696 (7)	C(64)	2005 (14)	2598 (10)	1384 (9)
C(35)	-5461 (14)	6483 (9)	-77 (8)	C(65)	2871 (15)	2870 (10)	1022 (9)
C(36)	-6444 (14)	6052 (9)	779 (8)	C(66)	1533 (15)	1683 (10)	1118 (9)

°C results in elimination of Me₃SiCl and formation of the unprecedented trigonal-bipyramidal cage compound P₂(*i*-Pr₂NB)₃. All attempts at that time, however, to prepare additional symmetric and asymmetric derivatives of P₂B₃ cages by this route failed. Since then, syntheses for diphosphadiboretane ring compounds (R₂NBPH)₂ have been developed,¹¹ and they appeared to offer a building block for the stepwise assembly of various cage structures including new examples in the P₂B₃ family.

Indeed, in the present study, we find that the monolithium salts **2** and **10** of the two symmetrical diphosphadiboretanes (*i*-Pr₂BNPH)₂, **1**, and (tmpBPH)₂, **9**, are useful reagents for the preparation of fully symmetric and asymmetric P₂(R₂NB)₃ cage compounds. The reaction scheme is summarized in eqs 1–5. Combinations of the lithium salts **2** and **10** with tmpBCl₂, (tms)₂NBCl₂, and *i*-Pr₂NBCl₂ result in the formation of the previously unreported 1-[chloro(dialkylamino)boryl]-1,3,2,4-diphosphadiboretanes **3**, **5**, **7**, and **11**, as shown in eq 2. These compounds are isolated in modest to good yield, and they are stable toward HCl elimination and rearrangement processes at room temperature. However, addition of *t*-BuLi to **3**, **5**, and **11** in hexane results in facile conversion to the new cage compounds **4**, **6**, and **12** that contain two different amino groups. The reaction with **7** with *t*-BuLi results in formation of the previously reported symmetrical compound **8** in 40% yield.⁶ It is also noted that utilization of the weaker base *n*-BuLi in the dehydrohalogenation reactions (eq 4) gives lower yields of the respective cage compounds. In contrast, combination of **10** with (tms)₂NBCl₂ in hexane with gentle heating leads to direct dehydrohalogenation with formation of **13**, but in low yield. Attempts to improve the yield of **13** by addition of Et₃N failed. The formation of **13**, as shown in eq 5, is also accompanied by production of the known bicyclic compound (tmpBP)₂.⁴ The reaction of **10** with tmpBCl₂

occurs without base promotion, and the symmetric cage **14** is produced in good yield without formation of bicyclic (tmpBP)₂.

The compounds **3–6**, **8**, and **11–14** display a parent ion in the mass spectra and appropriate fragment ions consistent with the proposed structures.¹⁷ Infrared spectra for **3**, **5**, and **11** show one or two weak absorptions in the P–H stretching vibration region:^{11,18} **3**, 2256 and 2237 cm⁻¹; **5**, 2266 cm⁻¹; and **11**, 2246 and 2232 cm⁻¹. These values compare favorably with the P–H stretching vibrations in **1**, 2267 cm⁻¹ and **9**, 2277 cm⁻¹. As expected, the cage compounds are free of infrared absorptions in this region.

The NMR data for the new compounds are summarized in Table V. The ³¹P{¹H} NMR spectra for **3**, **5**, and **11** display two resonances of equal intensity. The lower field resonances δ–108.1, –77.8, and –98.9 for **3**, **5**, and **11** of each pair may be assigned to the triborylphosphane fragment B₂PB', and the higher field resonances δ–126.9, –151.4, and –107.8 to the diborylphosphane fragment.^{11,18} These assignments are substantiated by observation of P–H coupling on the high-field resonance (¹J_{PH} = 191–194 Hz) in the proton-coupled ³¹P NMR spectra. The ¹¹B{¹H} NMR spectra for **3**, **5**, and **11** show two peaks in a 2:1 area ratio: **3**, δ 50.3 (Btmp, 1), 39.3 (BN-*i*-Pr₂, 2);¹⁹ **5**, δ 47.0 (BN-*i*-Pr₂, 2), 52.0 (BN(SiMe₃)₂, 1); **11**, δ 51.0 (Btmp, 2), 39.5 (BN-*i*-Pr₂, 1). The ³¹P and ¹¹B NMR data for **7** were not recorded since the compound was not isolated. The ³¹P{¹H} NMR spectra for the cage compounds **4**, **6**, **8**, **12**, **13**, and **14** show a single resonance in the range δ –13 to +70. The observed shift range may arise

(17) The mass spectrum and infrared spectrum of **7** were not recorded.

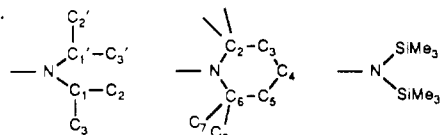
(18) Dou, D.; Wood, G. L.; Duesler, E. N.; Paine, R. T.; Nöth, H. *Inorg. Chem.* **1992**, *31*, 1695.

(19) A third broad ¹¹B{¹H} resonance centered at δ ~48.5, tentatively assigned to a presently unidentified byproduct, makes the accurate determination of the area ratio for **3** impossible.

Table V. NMR Data for Phosphinoboranes 1–17 (23 °C, C₆D₆)^a

compound	$\delta(^{31}\text{P})$	$\delta(^{11}\text{B})$ (intens)	$\delta(^1\text{H})$		$\delta(^{13}\text{C})$	
3	-108.1 -126.9	50.3 (2) 39.3 (1)	1.6		21.1	47.6
			1.5 (tmp)		22.4	47.1 (CH)
			1.2		23.3 (CH ₃)	
			1.1 (CH ₃)	4.9	24.7	
			1.0	4.0 (CH)	16.4, 33.6, 41.0, 58.1 (tmp)	
4	10.1	43.7 (1) 39.7 (2)	5.2 (PH)			
			1.25 (CH ₃)	3.8 (CH)	23.9 (CH ₃)	52.5 (CH)
			1.7		15.8, 33.4, 39.7, 57.0 (tmp)	
			1.53 (tmp)			
			1.51			
5	-77.8 -151.4	52.0 (1) 47.0 (2)	0.36 (tms)		3.8 (tms)	
			1.25	3.2	22.1	47.4
			1.13 (CH ₃)	4.3 (CH)	24.6 (CH ₃)	55.4 (CH)
			4.5 (PH)			
6	23.5	53.0 (1) 39.2 (2)	0.45 (tms)		4.5 (tms)	
			1.2 (CH ₃)	3.8 (CH)	23.7 (CH ₃)	53.0 (CH)
			1.2 (CH ₃)	3.9 (CH)	23.6 (CH ₃)	52.5 (CH)
8	-13.0	40.5	1.2 (CH ₃)	3.9 (CH)	23.6 (CH ₃)	52.5 (CH)
11	-98.9	51.0 (2)	1.0	3.1	20.9	47.1
11	-107.8	39.5 (1)	1.4 (CH ₃)	5.1 (CH)	22.9 (CH ₃)	53.9 (CH)
			1.59		16.5, 33.8, 41.3, 57.8 (tmp)	
			1.43 (tmp)			
			5.6 (PH)			
			1.3 (CH ₃)	3.9 (CH)	24.0 (CH ₃)	52.6 (CH)
12	32.0	42.8 (2) 38.6 (1)	1.7, 1.5 (tmp)		15.9, 33.6, 39.9, 57.0 (tmp)	
			0.46 (tms)		4.7 (tms)	
13	69.2	51.1 (1) 41.9 (2)	1.6		15.5, 33.5, 38.1, 56.9 (tmp)	
			1.5 (tmp)			
14 ^b	54.3	42.7	1.6		15.9, 33.9, 39.9, 57.1 (tmp)	
15	-25.7 -33.1	40.0 (1) 35.1 (2)	1.1	4.8	22.0	56.6
			1.2 (CH ₃)	3.1 (CH)	25.6 (CH ₃)	46.4 (CH)
			1.5, 1.4 (tmp)		14.7, 33.6, 36.6, 57.3 (tmp)	
16	-32.4 -56.8	50.9 (1) -33.1 (2)	0.36 (tms)		4.2 (tms)	
			1.17 (CH ₃)	5.1	22.0	46.4
			1.26	3.12 (CH)	25.6 (CH ₃)	56.2 (CH)
17	-24.5 -39.4	38.4 (2) 33.0 (1)	1.21	3.1	22.2 ^c	46.5
			1.30 (CH ₃)	5.5 (CH)	25.9 (CH ₃)	53.7 (CH)
			1.60, 1.59, 1.43, 1.36 (tmp)		14.8, 32.3, 35.4, 36.2, 57.7 (tmp)	

^a Coupling constant (Hz): (3) $^1J_{\text{PH}} = 192.8$, $^3J_{\text{PH}} = 14.9$; (4) $^4J_{\text{CP}} = 7.3$ (C_{7,8}), $^1J_{\text{HH}} = 6.7$ (C₂); (5) $^4J_{\text{CP}} = 2.1$ (C₂), $^3J_{\text{CP}} = 5.0$ (C₁), $^3J_{\text{CP}} = 5.1$, $^3J_{\text{HH}} = 6.8$ (C₂), $^3J_{\text{HH}} = 6.7$ (C₁), $^3J_{\text{HH}} = 6.7$ (C_{1'}), $^1J_{\text{PH}} = 191.5$, $^3J_{\text{PH}} = 9.2$; (6) $^4J_{\text{CP}} = 4.5$ (SiMe), $^3J_{\text{HH}} = 6.8$; (8) $^3J_{\text{CP}} = 5.2$ (C₁, *i*-Pr₂N), $^3J_{\text{HH}} = 6.7$ (C₁); (11) $^3J_{\text{CP}} = 16.6$ (C₁, *i*-Pr₂N), $^3J_{\text{CP}} = 4.3$ (C_{2,6}, tmp), $^3J_{\text{HH}} = 6.6$ (C₁), $^3J_{\text{HH}} = 7.0$ (C_{1'}), $^1J_{\text{PH}} = 193.6$, $^3J_{\text{PH}} = 13.8$; (12) $^4J_{\text{CP}} = 7.5$ (C_{7,8}), $^3J_{\text{HH}} = 6.7$ (C₂); (13) $^4J_{\text{CP}} = 6.8$ (C_{7,8}), $^4J_{\text{CP}} = 4.0$ (SiMe); (15) $^3J_{\text{CP}} = 4.2$ (C₁, *i*-Pr₂N), $^3J_{\text{CP}} = 2.7$ (C_{2,6}, tmp), $^3J_{\text{HH}} = 6.7$ (C₂, *i*-Pr₂N), $^3J_{\text{HH}} = 6.8$ (C_{2'}, *i*-Pr₂N); (16) $^3J_{\text{CP}} = 4.9$ (C₁, *i*-Pr₂N), $^4J_{\text{CP}} = 2.4$ (SiMe), $^3J_{\text{HH}} = 6.7$, $^3J_{\text{HH}} = 6.7$; (17) $^3J_{\text{CP}} = 5.7$ (C₁, *i*-Pr₂N), $^3J_{\text{CP}} = 3.9$ (C_{2,6}, tmp), $^3J_{\text{HH}} = 6.7$.



^b Sample dissolved in toluene-*d*₈. ^c Sample dissolved in CDCl₃.

from variations in the very acute bond angles at the phosphorus atoms *vide infra* and from a combination of electronic and steric effects introduced by the BNR₂ and BNR_{2'} fragments. The ¹¹B-{¹H} NMR spectra for the asymmetrically substituted cages show two resonances in a 2:1 ratio, and the intensities allow the assignment of the boron fragments in the following ranges:²⁰ BN-*i*-Pr₂, δ 38–47; BN(SiMe₃)₂, δ 51–53; Btmp, δ 41–51. The symmetrically substituted cage compounds **8** and **14** show a single boron resonance within the appropriate shift ranges.

The combinations of P₂(*i*-Pr₂NB)₃, **8**, with Fe₂(CO)₉, Cr(CO)₅NMe₃, and W(CO)₅NMe₃ were previously observed to form 1:1 adducts of the general types L·M(CO)_n.²¹ No evidence was found for the simultaneous coordination of both lone pairs. In the present study, the coordination chemistry of **4**, **6**, and **12** was examined, and this is summarized in eq 6. All attempts to

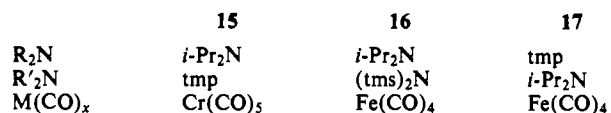
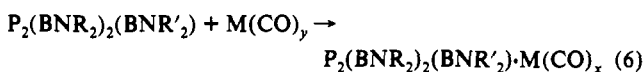
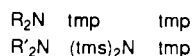
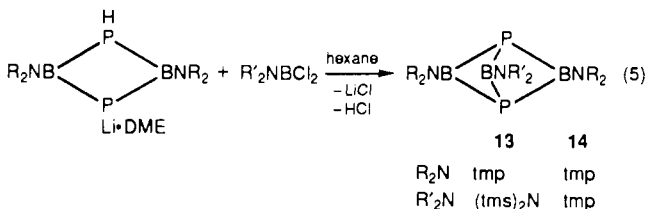
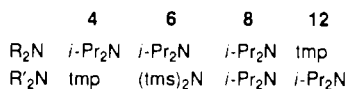
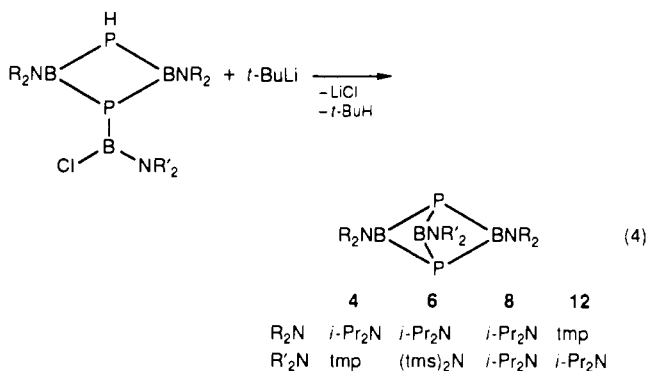
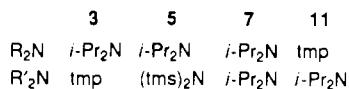
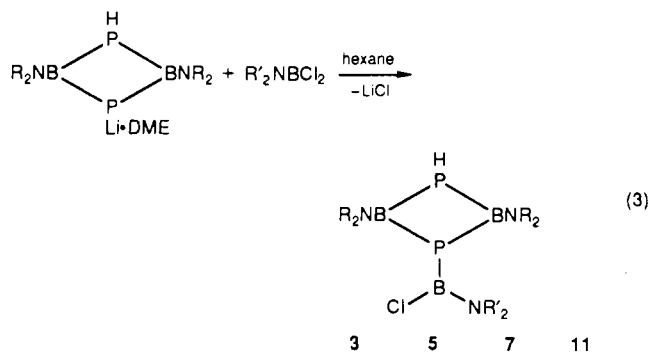
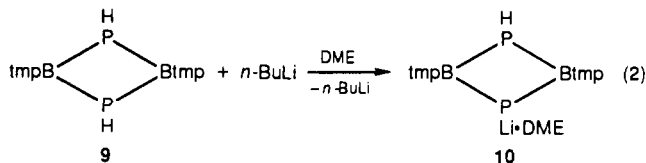
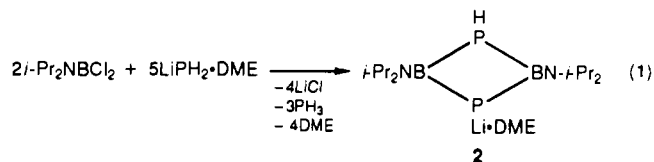
prepare bimetallic complexes failed. The mass spectrum of **16** shows a parent ion; however, the spectra of the other two complexes display only ions typical of the ligand and metal fragments. The infrared spectrum of **15** shows three bands in the carbonyl stretching region at 2053, 1954, and 1934 cm⁻¹, which are typical of M(CO)₅-L compounds.²² Furthermore, these data agree closely with the spectra for (CO)₅Cr·[P₂(*i*-Pr₂NB)₃]:²¹ 2053, 1956, and 1933 cm⁻¹. The infrared spectra in the carbonyl region for **16**, 2041, 1966, and 1935 cm⁻¹, and **17**, 2037, 1962, and 1933 cm⁻¹, are essentially identical with the carbonyl region of (CO)₄Fe·[P₂(*i*-Pr₂NB)₃],²¹ and all are consistent with the axially substituted (CO)₄Fe·L geometry.²²

The NMR data for the complexes are summarized in Table V. The ³¹P{¹H} NMR spectra display two resonances, both shifted upfield from the single resonance in the respective free ligands. In each case, the lower field resonance of the pair is broader than the higher field resonance, and the former is consequently assigned to the metal-coordinated phosphorus atom. Similar patterns and

(20) Nöth, H.; Wraackmeyer, B. In *Nuclear Magnetic Resonance Spectroscopy of Boron Compounds*; Diehl, P., Fluck, E., Kosfeld, R., Eds.; Springer-Verlag: Berlin, 1978.

(21) Wood, G. L.; Duesler, E. N.; Paine, R. T.; Nöth, H. *Phosphorus, Sulfur Silicon Relat. Elem.* **1989**, *41*, 267.

(22) Purcell, K. F.; Kotz, J. C. *Inorganic Chemistry*; W. B. Saunders Co.: Philadelphia, 1977; p 901.



assignments have been described for (CO)₅Cr·[P₂(BN-*i*-Pr₂)₃] and (CO)₄Fe·[P₂(BN-*i*-Pr₂)₃].²¹ The resonances for **15** and **16** appear as doublets with *J*_{PP} = 44.6 and 33.3 Hz, respectively. This coupling is not resolved in **17**. The ¹¹B NMR spectra show two resonances in a 2:1 ratio, each shifted 2–6 ppm upfield from the respective resonances in the free ligands. Similar upfield shifts were observed in the metal carbonyl complexes of **8**.²¹

The cage molecular structures of the ligands **6** and **14** and the complex **15** were confirmed by X-ray diffraction techniques. Views of the molecules are shown in Figures 1–3, and selected bond distances and angles are presented in Table VI. The molecular structures of **6** and **14** reveal a trigonal-bipyramidal P₂B₃ core

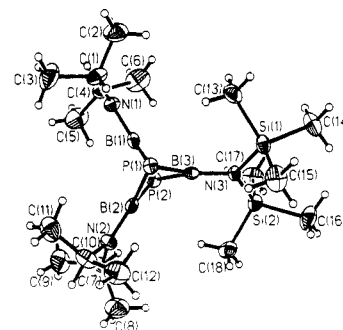


Figure 1. Molecular structure and atom-labeling scheme for P₂(*i*-Pr₂-NB)₂[(Me₃Si)₂NB] (**6**) (25% thermal ellipsoids).

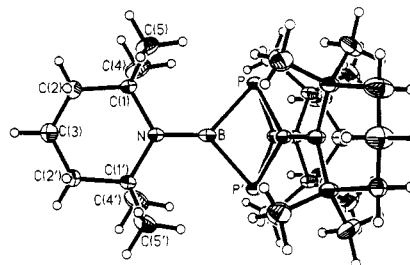


Figure 2. Molecular structure and atom-labeling scheme for P₂(tmpB)₃ (**14**) (25% thermal ellipsoids).

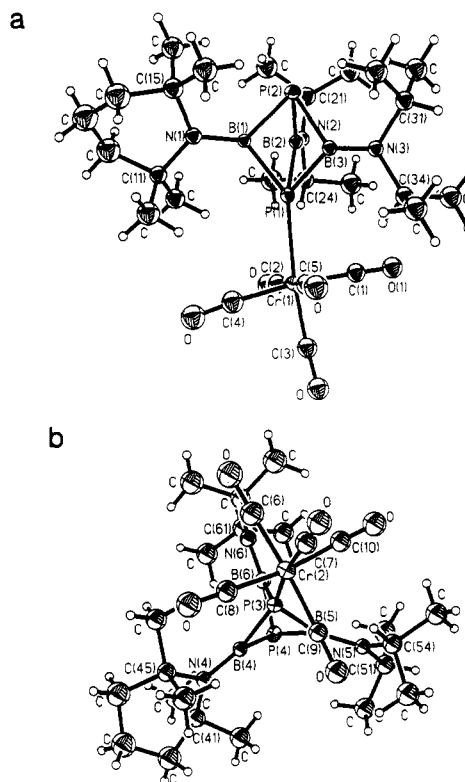


Figure 3. P₂(*i*-Pr₂NB)₂(tmpB)·Cr(CO)₅ (**15**) (25% thermal ellipsoids) shown in different orientations: (a) molecule 1; (b) molecule 2. Several atom labels are omitted for clarity.

that resembles the one found previously for P₂[*i*-Pr₂NB]₃,²¹ **8**. The molecule **14** possesses a C₃ axis and a perpendicular mirror plane, but no other symmetry elements. The B–P bond distances in **6** range from 1.935 (8) to 1.955 (7) Å (av distance 1.948 Å), and in **14** the distances are equivalent, 1.958 (4) Å. These compare favorably with the average P–B distance, 1.969 Å, in **8**. The exo B–N bond length in **6** spans from 1.382 (10) to 1.413 (8) Å, with the two shorter distances, 1.382 (10) and 1.386 (9) Å, associated with the BN-*i*-Pr₂ groups and the longer distance, 1.413 (8) Å, associated with the BN(SiMe₃)₂ group. These distances compare with the B–N distance, 1.34 (2) Å, in **8**. The dihedral angles between the planes defined by P(1)P(2)B(1)–N(1)C(1)C(4),

Table VI. Selected Bond Distances (Å) and Bond Angles (deg) for $P_2[i-Pr_2NB]_2[(Me_3Si)_2NB]$, **6**, $P_2(tmp)_3$, **14**, and $(CO)_5Cr\{Pr_2[i-Pr_2NB]_2[tmpB]\}$, **15**

	6	14	15
		Bond Lengths	
B-P	1.935 (8) P(1)-B(1) 1.953 (7) P(1)-B(2) 1.954 (7) P(1)-B(3) 1.951 (7) P(2)-B(1) 1.939 (7) P(2)-B(2) 1.955 (7) P(2)-B(3)	1.958 (4) P-B 1.958 (6) P-B' 1.959 (3) P-B'' 1.958 (4) P'-B'	1.974 (15) P(1)-B(1) 1.941 (17) P(1)-B(2) 1.938 (17) P(1)-B(3) 1.900 (16) P(2)-B(1) 1.955 (18) P(2)-B(2) 1.936 (14) P(2)-B(3) 1.982 (18) P(3)-B(4) 1.943 (17) P(3)-B(5) 1.944 (17) P(3)-B(6) 1.938 (14) P(4)-B(4) 1.928 (19) P(4)-B(5) 1.902 (19) P(4)-B(6)
B-N	1.382 (10) B(1)-N(1) 1.386 (9) B(2)-N(2) 1.413 (8) B(3)-N(3)	1.407 (6) B-N	1.427 (18) B(1)-N(1) 1.361 (22) B(2)-N(2) 1.399 (16) B(3)-N(3) 1.387 (19) B(4)-N(4) 1.395 (23) B(5)-N(5) 1.387 (22) B(6)-N(6)
P-Cr			2.473 (5) Cr(1)-P(1) 2.500 (3) Cr(2)-P(3)
Cr-CO (av)			1.847 Cr(1)-C 1.831 Cr(2)-C
		Bond Angles	
B-P-B	67.0 (3) B(1)-P(1)-B(2) 67.9 (3) B(1)-P(1)-B(3) 68.7 (3) B(2)-P(1)-B(3) 67.0 (3) B(1)-P(2)-B(2) 67.6 (3) B(1)-P(2)-B(3) 69.0 (3) B(2)-P(2)-B(3)	71.4 (2) B-P-B' 71.4 (2) B-P-B'' 71.4 (2) B'-P-B''	68.4 (7) B(1)-P(1)-B(2) 74.4 (6) B(1)-P(1)-B(3) 70.1 (7) B(2)-P(1)-B(3) 69.7 (7) B(1)-P(2)-B(2) 76.2 (6) B(1)-P(2)-B(3) 69.8 (7) B(2)-P(2)-B(3) 72.1 (7) B(4)-P(3)-B(5) 69.0 (7) B(4)-P(3)-B(6) 71.1 (8) B(5)-P(3)-B(6) 73.4 (7) B(4)-P(4)-B(5) 70.7 (7) B(4)-P(4)-B(6) 72.4 (8) B(5)-P(4)-B(6) 95.3 (7) P(1)-B(1)-P(2) 94.6 (8) P(1)-B(2)-P(2) 95.3 (6) P(1)-B(3)-P(2) 93.9 (7) P(3)-B(4)-P(4) 95.4 (9) P(3)-B(5)-P(4) 96.3 (8) P(3)-B(6)-P(4)
P-B-P	100.1 (4) P(1)-B(1)-P(2) 99.9 (3) P(1)-B(2)-P(2) 99.2 (3) P(1)-B(3)-P(2)	95.3 (2) P-B-P'	

P(1)P(2)B(2)-N(2)C(7)C(10), and P(1)P(2)B(3)-N(3)Si(1)-Si(2) in **6** are 2.2°, 6.9°, and 28.6°, respectively. These angles and the B-N bond distances are consistent with a greater degree of B-N π bonding in a BN-*i*-Pr₂ group compared to a BN(SiMe₃)₂ group where the silicon is expected to competitively dominate π bonding with nitrogen.²³ The B-N bond distance in **14** is 1.407 (6) Å, and the PP'B-NC(1)C(1') dihedral angle is 12.8°. The average B-P-B angles in **6**, 67.9°, and **14**, 71.4, are highly compressed for a phosphane, and they are similar to the value of 68.9 (2)° in **8**. The average P-B-P bond angles in **6**, 99.7°, and in **14**, 95.3°, are also similar to the value of 98.5 (5)° in **8**.

The monometallic complex **15** crystallizes with two independent molecules in the unit cell. The structure shows that the Cr(CO)₅ fragment is bonded to one of the phosphorus atoms of the ligand **4**. The average Cr-P bond distance, 2.486 (22) Å, is relatively long, compared with the Cr-P distances in (CO)₅Cr-PPh₃, 2.422 (1) Å,²⁴ [tmpBPH]₂-Cr(CO)₅,¹¹ 2.458 (2) Å, and (CO)₅Cr-P(H)[(*i*-Pr₂N)₂B]₂,¹⁸ 2.451 (1) Å. The bond length in **15**, however, is shorter than the Cr-P distance (2.517 (2) Å) in (CO)₅Cr-P(H)[(*i*-Pr₂N)₂B][tmpB(Cl)].¹⁸ The P-B bond distances span a wide range, 1.900 (16) to 1.982 (18) Å, with an average distance, 1.940 Å, which is comparable with the P-B distances in the free ligands **6**, **8**, and **14**. The B-N bond distance ranges from 1.361 (22) to 1.427 (18) Å, and the dihedral angles involving the tmp

fragment (at the B(1)-N(1) and B(4)-N(4) bonds), 22.6° and 23.8°, are much larger than those involving the *i*-Pr₂N groups, 2.7°, 2.3°, 7.0°, and 0.7°. Once more, this is indicative of better B-N π overlap in the BN-*i*-Pr₂ groups. The average B-P-B bond angle for the coordinated phosphorus atom is 70.7°, and the angle involving the uncoordinated phosphorus atom is 72.1°.

Conclusion

The availability of diphosphadiboretane ring compounds provides access to a number of unique P₂(BNR₂)₃ cage compounds. The stepwise assembly process utilized in the synthesis suggests that additional examples of five and six atom cages, P₂(BNR₂)₂X and P₂(BNR₂)₂X₂, might be accessible, and our success in preparing such compounds will be described in a subsequent paper.

Acknowledgment is made to the National Science Foundation (Grant CHE-8503550) (R.T.P.) and the Fonds der Chemischen Industrie (H.N.). A NATO grant allowed the cooperation of our research groups. Support from the Department of Energy URIP (Grant DE-FG05-86ER75294) assisted in the purchase of the JEOL GSX-400 NMR spectrometer, and funds from the NSF (Grant CHE-8807358) supported the purchase of the Bruker WP-250 spectrometer.

Supplementary Material Available: Tables S-1-S-5, giving full descriptions of the X-ray analyses, anisotropic thermal parameters, hydrogen atom positional parameters, and full listings of bond distances and bond angles and ORTEP diagrams (35 pages); listings of calculated and observed structure factors (42 pages). Ordering information is given on any current masthead page.

(23) Greenwood, N. N.; Earnshaw, A. *Chemistry of the Elements*; Pergamon Press: New York, 1984; p 418. The related dihedral angles in P₂[*i*-Pr₂NB]₃ have not been calculated and compared to those in **6** since there is an orientational disorder in the *i*-Pr groups in **8**.⁶

(24) Plastos, H. J.; Stewart, J. M.; Grim, S. O. *Inorg. Chem.* **1973**, *12*, 265.